

BFKL Pomeron calculus: solution to equations for nucleus-nucleus scattering in the saturation domain

Carlos Contreras^a, Eugene Levin^{a,b} and Rodrigo Meneses^c

^a *Departamento de Física, Universidad Técnica Federico Santa María and Centro Científico-Tecnológico de Valparaíso, Avda. España 1680, Casilla 110-V, Valparaíso, Chile*

^b *Department of Particle Physics, School of Physics and Astronomy, Tel Aviv University, Tel Aviv, 69978, Israel*

^c *Escuela de Ingeniería Civil, Facultad de Ingeniería, Universidad de Valparaíso, Avda Errazuriz 1834, Valparaíso, Chile*

ABSTRACT: In this paper we solve the equation for nucleus-nucleus scattering in the BFKL Pomeron calculus, suggested by Braun [1]. We find these solutions analytically at high energies as well as numerically in the entire region of energies inside the saturation region. The semi-classical approximation is used to select out the infinite set of the parasite solutions. The nucleus-nucleus cross sections at high energy are estimated and compared with the Glauber-Gribov approach. It turns out that the exact formula gives the estimates that are very close to the ones based on Glauber-Gribov formula which is important for the practical applications.

KEYWORDS: BFKL Pomeron calculus, semi-classical approach, Pomeron action, equations of motion.

PACS: 13.85.-t, 13.85.Hd, 11.55.-m, 11.55.Bq

Contents

1. Introduction	1
2. The BFKL Pomeron calculus for nucleus-nucleus interaction at high energy	2
2.1 Equations for nucleus-nucleus scattering	2
2.2 Solution inside the saturation domain: general approach	5
2.3 Asymptotic solution	6
3. Semiclassical solution for $\phi(z, Y')$	7
3.1 Equations	7
3.2 Solutions in Ω_1	8
3.3 Solutions in Ω_2	10
4. Asymptotic solution with $\gamma \longrightarrow z_Y / \left(\bar{\alpha}_S \frac{\chi(\gamma_{cr})}{1-\gamma_{cr}} \right)$	10
5. Nucleus-nucleus scattering amplitude	12
6. Conclusions	17
7. Acknowledgements	19

1. Introduction

The goal of this paper is to find the solution to the equations for nucleus-nucleus collision that have been derived in Ref. [1]. We continue the attempts, taken in Refs. [2–5], to study these equations and to search the general method of solving them.

Nucleus-nucleus scattering gives the most informative example of dense - dense parton system interactions in which we can see the main prediction of Color Glass Condensate/saturation approach [7–12]. However, in spite of the fact that we know quite well qualitative features of nucleus-nucleus scattering (see Refs. [13]) CGC/saturation approach suffers by the absence of the evolution equation that gives us a possibility to find the scattering amplitude at high energy. On the other hand we know quite well the

initial condition for such an evolution [9]. Fortunately, the second approach to the high energy QCD; the BFKL [14, 15] Pomeron calculus, gives the equations for nucleus-nucleus scattering at high energy. For dilute-dense parton system scattering both approaches: BFKL Pomeron calculus and Color Glass Condensate (CGC), lead to the same nonlinear equations [1, 16]. Therefore, we can hope that the equations given by BFKL Pomeron calculus would be proven in the framework of CGC.

In the next section we give the brief review of the equations derived in Ref. [1] and discuss their main properties. This section does not contain any new results except section 2.3, and it is written for the completeness of presentation. In section 2.3 we consider the asymptotic solution to the problem at large values of rapidity Y in the framework of the semiclassical approach that has been developed by us in Refs. [4, 5]. In the next section we show that the number of possible solutions has to be reduce to unique solution which is discussed in section 5. In section 6 we derive that nucleus-nucleus amplitude for the solution given in section 5. In conclusions we summarize our results and compare our solution with the numerical solutions of Refs. [2, 3]. Unfortunately, the main equations were proposed a decade ago but we have only had five papers devoted to a search of the solutions (see Refs. [2–5] and this paper).

2. The BFKL Pomeron calculus for nucleus-nucleus interaction at high energy

2.1 Equations for nucleus-nucleus scattering

The most economic and elegant form the BFKL Pomeron calculus has in terms of the functional integral [1]

$$Z[\Phi, \Phi^+] = \int D\Phi D\Phi^+ e^S \quad \text{with} \quad S = S_0 + S_I + S_E \quad (2.1)$$

where S_0 describes free Pomerons, S_I corresponds to their mutual interaction while S_E relates to the interaction with the external sources (target and projectile).

We will write these actions in the momentum representation [2, 5] which is defined as

$$\Phi^\dagger(x_1, x_2, Y') = \Phi^\dagger(x_{12}, b, Y') = x_{12}^2 \int d^2 k_1 e^{-ik_1 \cdot x_{12}} \Phi^\dagger(k_1, b, Y') \quad (2.2)$$

$$\Phi(x_1, x_2, Y') = \Phi(x_{12}, b, Y') = x_{12}^2 \int d^2 k_2 e^{ik_2 \cdot x_{12}} \Phi(k_2, b, Y') \quad (2.3)$$

S_0 takes the form

$$S_0 = 64(2\pi)^2 \int dY' \int d^2 b \int d^2 k \Phi^\dagger(k, b, Y') \left\{ \left(\frac{\partial}{\partial l} + 1 \right)^2 \frac{\partial^2}{\partial l^2} \left\{ \frac{\partial}{\partial Y'} - \mathcal{H} \right\} \Phi(k, b, Y') \right\} \quad (2.4)$$

where $l = \ln k^2$ and

$$\mathcal{H}\Phi(k, b, Y) = \bar{\alpha}_S \left\{ \int \frac{d^2 k'}{(\vec{k} - \vec{k}')^2} \Phi(k', b, Y) - \frac{1}{2} \int \frac{k^2 d^2 k'}{k'^2 (\vec{k} - \vec{k}')^2} \Phi(k, b, Y) \right\} \quad (2.5)$$

where $\bar{\alpha}_S = (N_c/\pi) \alpha_S$ (N_c is the number of colours and the running QCD coupling $\alpha_S = 1/(\beta_0 \ln(k^2/\Lambda_{QCD}^2))$) and $\beta_0 = (33 - 2n_f)/12\pi$ with n_f is the number of the fermions).

The interaction term S_I can be written as follows [5]:

$$S_I = 16 \frac{(2\pi)^5 \bar{\alpha}_S^2}{N_c} \int dY' \int 4d^2b \int d^2k \left\{ \Phi^\dagger(-k, b, Y') \Phi^\dagger(-k, b, Y') \left(\frac{\partial}{\partial l} + 1 \right)^2 \frac{\partial^2}{\partial l^2} \Phi(k, b, Y') \right. \\ \left. + \Phi(-k, b, Y') \Phi(-k, b, Y') \left(\frac{\partial}{\partial l} + 1 \right)^2 \frac{\partial^2}{\partial l^2} \Phi^\dagger(k, b, Y') \right\} \quad (2.6)$$

The equations for nucleus-nucleus scattering have been derived from the averaging of the equations of motion for the action of Eq. (2.1)

$$\left\langle \frac{\delta S}{\delta \Phi(k, b, Y')} \right\rangle = 0 \quad \left\langle \frac{\delta S}{\delta \Phi^\dagger(k, b, Y')} \right\rangle = 0 \quad (2.7)$$

where averaging is understood as

$$\langle O(x, z; Y') \rangle \equiv \frac{\int D\Phi D\Phi^\dagger O(k, b, Y') e^{S[\Phi, \Phi^\dagger]}}{\int D\Phi D\Phi^\dagger e^{S[\Phi, \Phi^\dagger]}|_{S_E=0}} \quad (2.8)$$

Deriving the equation of motion we assume that

$$\begin{aligned} \langle \Phi^2(k, Y'; b) \rangle &= \left(\langle \Phi(k, Y'; b) \rangle \right)^2 \\ \langle (\Phi^\dagger)^2(k, Y'; b) \rangle &= \left(\langle \Phi^\dagger(k, Y'; b) \rangle \right)^2 \\ \langle \Phi(k, Y'; b) \Phi^\dagger(k, Y'; b) \rangle &= \langle \Phi(k, Y'; b) \rangle \times \langle \Phi^\dagger(k, Y'; b) \rangle \end{aligned} \quad (2.9)$$

These identities are proven in the case of nucleus-nucleus scattering within accuracy of about $1/A^{1/3}$ (see Refs. [1, 4, 11]). We need to find the relation between fields $\Phi(k, b, Y')$ and $\Phi^\dagger(k, b, Y')$ and the scattering amplitude owing to the single BFKL Pomeron exchange for $S_I = 0$ which we denote $N(k, k_0; b, Y')$ (where k and k_0 is the final and initial transverse momenta at rapidity Y and Y_0 , respectively).

Taking into account Eq. (2.9) one can see that the variation with respect to $\Phi^\dagger(k, b, Y')$ leads to the following equation of motion

$$\begin{aligned} \delta(S_0 + S_I)/\delta \Phi^\dagger(k, b, Y') &= 64(2\pi)^2 \left(\frac{\partial}{\partial l} + 1 \right)^2 \frac{\partial^2}{\partial l^2} \left(\frac{\partial}{\partial Y'} - H \right) \Phi(k, b, Y') \\ + 16 \left(\frac{2\pi \bar{\alpha}_S^2}{N_c} \right) (2\pi)^4 &\left\{ 2\Phi^\dagger(-k, b, Y') \left(\frac{\partial}{\partial l} + 1 \right)^2 \frac{\partial^2}{\partial l^2} \Phi(k, b, Y') + \left(\frac{\partial}{\partial l} + 1 \right)^2 \frac{\partial^2}{\partial l^2} \Phi^2(-k, b, Y') \right\} = 0 \end{aligned} \quad (2.10)$$

Using S_0 we easily see that

$$N(k, k_0, b; Y; Y_0) = 2\pi^2 \alpha_S \langle \Phi(l, b, Y - Y_0) \rangle \quad (2.11)$$

For understanding the relation between field Φ^\dagger and $N(k, K_0, b; Y; Y_0)$ where K_0 is the transverse momentum at rapidity Y we use the equation [7, 17]

$$N(K_0, k_0, b; Y; Y_0) = \int d^2 b' dl N^\dagger(K_0, k, \vec{b} - \vec{b}', Y - Y') N(k, k_0, \vec{b}', Y' - Y_0) \quad (2.12)$$

Eq. (2.12) has more general meaning than for exchange of one Pomeron (see Ref. [4] for proof in the case of nucleus-nucleus scattering): it gives the analytical continuation of the t -channel unitarity at large values of energy. For the BFKL Pomeron exchange we have

$$\begin{aligned} N_{\mathcal{P}}(K_0, k_0, b; Y; Y_0) &= N_{\mathcal{P}}(L, b, Y) = \int \frac{d\gamma}{2\pi i} n_{\mathcal{P}}(\gamma, b) e^{\bar{\alpha}_S \chi(\gamma) Y - (1-\gamma)L} \\ &= \int d^2 b' \int dl \int \frac{d\gamma^\dagger}{2\pi i} \int \frac{d\gamma}{2\pi i} n_{\mathcal{P}}^\dagger(\gamma^\dagger, \vec{b} - \vec{b}') e^{\bar{\alpha}_S \chi(\gamma) (Y - Y') - (1-\gamma^\dagger)(L-l)} n_{\mathcal{P}}(\gamma, b') e^{\bar{\alpha}_S \chi(\gamma') Y' - (1-\gamma')l} \end{aligned} \quad (2.13)$$

where $L = \ln(K_0^2/k_0^2)$ and $l = \ln(k^2/k_0^2)$. K_0 and k_0 are the momenta of the dipoles in the projectile and the target, respectively. Integrating over l we obtain that $\gamma^\dagger = \gamma$. Considering $Y' = Y_0$ we obtain that

$$N^\dagger(L, l, b; Y; Y_0) = 2\pi^2 \alpha_S \langle \Phi^\dagger(L - l, b, Y - Y_0) \rangle_{S_l=0} = N(b; L - l, Y - Y_0) \quad (2.14)$$

Assuming that Eq. (2.13) and Eq. (2.14) hold in the general case but not only for the BFKL Pomeron exchange, we reduce Eq. (2.10) to the following equation for the amplitudes

$$\begin{aligned} 0 &= \left(\frac{\partial}{\partial l} + 1 \right)^2 \frac{\partial^2}{\partial l^2} \left(\frac{\partial}{\partial Y'} - \mathcal{H} \right) N(l, b, Y') \\ &+ \bar{\alpha}_S \left\{ 2 N(L - l, b, Y - Y') \left(\frac{\partial}{\partial l} + 1 \right)^2 \frac{\partial^2}{\partial l^2} N(l, b, Y') + \left(\frac{\partial}{\partial l} + 1 \right)^2 \frac{\partial^2}{\partial l^2} N^2(l, b, Y') \right\} \end{aligned} \quad (2.15)$$

The second equation that stems from variation with respect to $\Phi(l, b, Y')$ has the same form as Eq. (2.15).

In Ref. [5] we solve Eq. (2.15) in semi-classical approximation assuming that

$$N(l, b, Y') = e^{S(l, b, Y')} = e^{\omega(l, b, Y') Y' - (1-\gamma(l, b, Y')) l} \quad (2.16)$$

and using the method of characteristics. In Eq. (2.16) we consider that $\omega(l, b, Y') = \partial S(l, b, Y') / \partial Y'$ and $\gamma(l, b, Y') = \partial S(l, b, Y') / \partial l$ are smooth functions of Y' and l (see Ref. [5] for more details). We found that for any value of z_Y there exists the solution at large l which is very close to the solution of the linear BFKL equation. In particular this solution has a critical characteristic for $\gamma = \gamma_{cr}$ that can be found from the following equation [7, 18]

$$\frac{\chi(\gamma_{cr})}{1 - \gamma_{cr}} = -\frac{d\chi(\gamma_{cr})}{d\gamma_{cr}} \quad \text{where} \quad \chi(\gamma) = 2\psi(1) - \psi(\gamma) - \psi(1 - \gamma) \leftarrow \text{kernel of the BFKL equation} \quad (2.17)$$

with $\psi(z) = d \ln \Gamma(z)/dz$ and $\Gamma(z)$ is the Euler gamma-function.

The equation for the saturation scale looks as follows

$$z \equiv \ln \left(\frac{Q_s^2(Y'; b)}{k^2} \right) = \bar{\alpha}_S \frac{\chi(\gamma_{cr})}{1 - \gamma_{cr}} Y' - l \quad (2.18)$$

In the vicinity of the saturation scale but for $z < 0$ the scattering amplitude shows the geometric scaling behaviour [19] i.e. it depends only on one variable (z) instead of three: Y' , l and b . For the Balitsky-Kovchegov equation the geometric scaling behaviour of the scattering amplitude is the typical feature inside the saturation region (see Ref. [20, 21]). In this paper we are going to solve Eq. (2.15) treating $N(z; Y')$ as a function of two variable: z (see Eq. (2.18)) and Y' . The choice of the variable shows that we believe that the scattering amplitude inside the saturation region has the geometric scaling behaviour and the initial condition for this solution can be found from the solution outside of the saturation scale, namely,

$$N(z=0, Y') = N_0; \quad \frac{dN(z)}{dz} \Big|_{z=0} = (1 - \gamma_{cr}) N_0 = 1 - e^{-\phi_0} \quad (2.19)$$

Recall that on the critical trajectory, the amplitude is constant and in the vicinity of the saturation scale it is proportional to $N_0 \exp \left((1 - \gamma_{cr}) z \right)$. However, introducing a dependence on Y' we are going to check whether the assumption on the scaling behavior of the amplitude is correct and within what accuracy. The initial conditions at $Y' = 0$ we set using the McLerran - Venugopalan formula [9] (see term $\{\dots\}$ below), namely

$$N(z, Y' = 0) = \int \frac{d^2 x_{12}}{x_{12}^2} \left\{ 1 - e^{-Q_s(Y'=0) x_{12}^2/4} \right\} = \frac{1}{2} \Gamma(0, k^2/Q_s^2(Y' = 0)) \quad (2.20)$$

2.2 Solution inside the saturation domain: general approach

For finding the solution inside the saturation region we will use a method proposed in Ref. [21] (see also Refs. [5, 6]): we introduce function $\phi(z)$ as follows

$$N(z, Y') = \frac{1}{2} \int_0^z dz' \left(1 - e^{-\phi(z', Y')} \right) + N_0 \quad (2.21)$$

and assuming that function $\partial\phi(z, Y')/\partial z$ is a smooth function we will find the solution to Eq. (2.15).

The smoothness of function $\partial\phi(z, Y')/\partial z$ means that

$$\left(\frac{\partial}{\partial z} \right)^n N(z, Y') = \frac{1}{2} \left(\frac{\partial}{\partial z} \right)^{n-1} \left(1 - e^{-\phi(z, Y')} \right) = \frac{1}{2} \left(-\frac{\partial\phi(z)}{\partial z} \right)^{n-1} e^{-\phi(z, Y')} \quad (2.22)$$

Using Eq. (2.22) as well as the properties of the BFKL equation (see Ref. [5] for details) we obtain the following equation

$$\tilde{\omega} + \mathcal{L}(\gamma) - \mathcal{F}(\gamma) e^{-\phi(z)} = 2N(z, Y') + 2N^\dagger(z, Y') = 2N(z, Y') + 2N^\dagger(z_Y - z, Y - Y') \quad (2.23)$$

Where

$$\gamma = \frac{\partial \phi(z, Y')}{\partial z} \quad \text{and} \quad \tilde{\omega} = \frac{\partial \phi(z, Y')}{\tilde{\alpha}_S \partial Y'}; \quad (2.24)$$

$$\phi(z=0, Y') = (1 - \gamma_{cr}) N_0 = 0.63 N_0 \quad \text{and} \quad \phi(z, Y'=0) = \phi_0 e^z; \quad (2.25)$$

$$\mathcal{L}(\gamma) = \frac{\chi(\gamma_{cr})}{1 - \gamma_{cr}} \gamma + \chi(\gamma) - \frac{1}{\gamma} + \frac{1 + 3\gamma}{\gamma(1 + \gamma)}; \quad (2.26)$$

$$\mathcal{F}(\gamma) = \frac{1 + 6\gamma + 7\gamma^2}{\gamma(1 + \gamma)^2}; \quad (2.27)$$

Introducing $\tilde{N} = 2N$ we can rewrite Eq. (2.23) in the form

$$\begin{aligned} & \frac{\tilde{N}_{zY'}''(z, Y')}{(1 - \tilde{N}'_z(z, Y'))} = \\ & \mathcal{L}\left(\frac{\tilde{N}_{zz}''(z, Y')}{(1 - \tilde{N}'_z(z, Y'))}\right) - \mathcal{F}\left(\frac{\tilde{N}_{zz}''(z, Y')}{(1 - \tilde{N}'_z(z, Y'))}\right) (1 - \tilde{N}'_z(z, Y')) - \tilde{N}(z, Y') - \tilde{N}(z_Y - z, Y - Y') \end{aligned} \quad (2.28)$$

Initial conditions for this equation are given by Eq. (2.25).

2.3 Asymptotic solution

Demonstrating the main features and the problems that we face solving Eq. (2.23) we, first, investigate the specific case: $\phi(z, Y')$ increases at large z and it has a geometric scaling behaviour $\phi(z, Y') = \phi(z)$. Using these assumptions we can simplify the general equation (see Eq. (2.23)):

$$\mathcal{L}(\gamma) = 2N(z) + 2N(z_Y - z) = z_Y \quad (2.29)$$

Function $\mathcal{L}(\gamma = d\phi/dz)$ is shown in Fig. 1 (black line). One can see that we have the following asymptotic solutions [5]:

1. For $z_Y > z_Y^{\min} \approx 6.3$ there is a solution at $\phi'_z(z) = \gamma(z) \ll 1$ ($\gamma \rightarrow 0$);
2. For all z_Y we have solutions $\phi'(z) = n z$ ($\gamma \rightarrow n$), where $n = 1, 2, 3, \dots$;
3. For $z_Y > z_Y^{\min} \approx 6.3$ we have the following solution:

$$\phi(z) = \frac{1 - \gamma_{cr}}{\chi(\gamma_{cr})} z_Y z \quad (2.30)$$

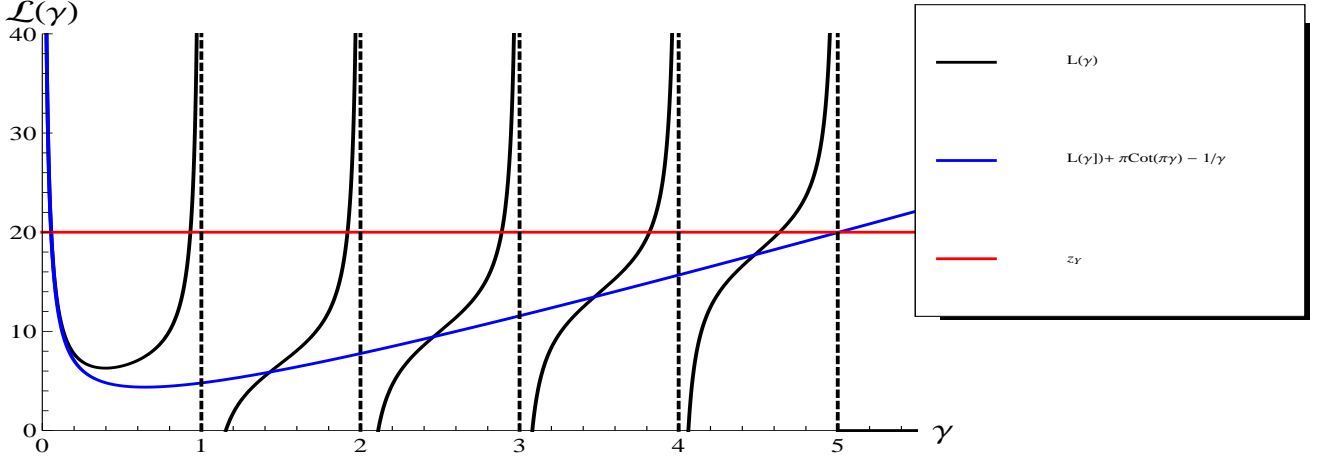


Figure 1: Function $\mathcal{L}(\gamma = d\phi(z)/dz)$ versus γ (black line). Blue curve shows $\mathcal{L}(\gamma) + \pi \cot(\pi\gamma) - 1/\gamma$ while the red one shows $\mathcal{L}(\gamma) = z_Y$.

In Fig. 1 the blue solid line shows

$$\tilde{\mathcal{L}} \equiv \mathcal{L}(\gamma) + \pi \cot(\pi\gamma) - 1/\gamma. \quad (2.31)$$

All poles at $\gamma = n$ are excluded in this function while the behaviour at large γ this function has the same as $\mathcal{L}(\gamma)$. This asymptotic behaviour at γ close to $z_Y/C(\gamma_{cr})$ can be translated in Eq. (2.30) (see also below Eq. (4.6) and Eq. (4.9)).

Therefore, one can see that we face two major problems in searching the solution: (i) at first sight we have infinite number of solutions even in this simplified case; and (ii) we need to find the solution if we exclude the singularities in $\mathcal{L}(\gamma)$.

The infinite number of solutions contradicts the common sense intuition that the physical problem has the only one solution being formulated correctly. In the next section 3 we show mathematical arguments that will discriminate different solutions and will select the only one solution. This physical solution will be found in section 4.

3. Semiclassical solution for $\phi(z, Y')$

3.1 Equations

For large $\phi(z, Y')$ Eq. (2.23) can be re-written in the form*

$$\tilde{\omega} + \mathcal{L}(\gamma) - \mathcal{F}(\gamma)e^{-\phi} - z_Y = \tilde{\omega} + \mathcal{G}(\gamma, \phi) - z_Y = 0 \quad (3.1)$$

*We will denote below by z_Y the sum $z_Y + 4N_0$ and hope it will not cause any difficulties in understanding.

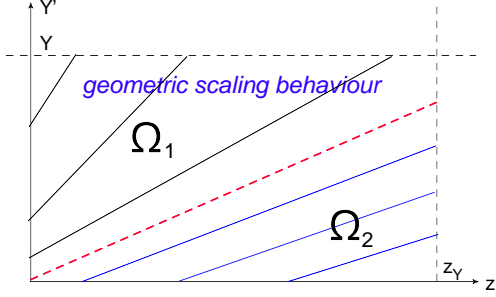


Figure 2: Two kinematic regions: Ω_1 and Ω_2 . The solid lines describe two sets of trajectories in Ω_1 and Ω_2 . The trajectories in Ω_1 start at $z = 0$ with given value of ϕ_0 . The trajectories in Ω_2 start at any point of z at $Y' = 0$. The initial value of $\gamma_0 = \phi_0 \exp(z_0)$. The dotted red line is the common characteristic line for both Ω_1 and Ω_2 . It has the form (see Eq. (4.5) and Eq. (4.4) below): $Y' = z/C(\gamma_{cr})$.

We solve this equation in semi-classical approximation assuming that $\phi(z, Y')$ is a smooth function of both variables z and Y' . It is known (see Refs. [22] and references therein) that for the equation in the form

$$F(Y', z, \phi, \gamma, \tilde{\omega}) = 0 \quad (3.2)$$

with smooth ϕ . We can introduce the set of characteristic lines : $z(t), Y'(t), \phi(t), \tilde{\omega}(t)$, and $\gamma(t)$ which are the functions of the variable t (artificial time), that satisfy the following equations:

$$\begin{aligned} (1.) \quad \frac{dz}{dt} &= F_\gamma = \frac{\partial \mathcal{G}(\gamma, \phi)}{\partial \gamma} \\ (2.) \quad \frac{dY'}{dt} &= F_{\tilde{\omega}} = 1 \\ (3.) \quad \frac{d\tilde{\phi}}{dt} &= \gamma F_\gamma + \tilde{\omega} F_{\tilde{\omega}} = \gamma \frac{\partial \mathcal{G}}{\partial \gamma} + \tilde{\omega} \\ (4.) \quad \frac{d\gamma}{dt} &= -(F_z + \gamma F_\phi) = -\gamma \mathcal{F}(\gamma) e^{-\phi} \\ (5.) \quad \frac{d\tilde{\omega}}{dt} &= -(F_{Y'} + \tilde{\omega} F_\phi) = -\tilde{\omega} \mathcal{F}(\gamma) e^{-\phi} \end{aligned} \quad (3.3)$$

From Eq. (3.3)-2 one can see that we can introduce $t = Y'$. Taking the ration of Eq. (3.3)-4 to Eq. (3.3)-5 we obtain that

$$\tilde{\omega}(Y') = \mathcal{K}(\gamma_0) \gamma(Y') \quad (3.4)$$

where $\gamma_0 \equiv \gamma(Y' = 0)$ is the initial value of γ which has to be found from the initial conditions.

Plugging Eq. (3.4) into Eq. (3.1) we reduce the system of equation (see Eq. (3.3)) to the following set of the equations:

$$e^{-\phi} = \left(\mathcal{L}(\gamma) - z_Y + \gamma \mathcal{K}(\gamma_0) \right) / \mathcal{F}(\gamma); \quad (3.5)$$

$$dz(Y')/dY' = \mathcal{L}_\gamma(\gamma) - \mathcal{F}_\gamma(\gamma) e^{-\phi}; \quad (3.6)$$

$$d\gamma/dY' = -\gamma \left(\mathcal{L}(\gamma) + \mathcal{K}(\gamma_0) \gamma - z_Y \right) \equiv T(\gamma, \gamma_0); \quad (3.7)$$

It turns out the general set of trajectories can be divided in two groups: the trajectories that start at $z = 0$ and at arbitrary Y' (the vertical axis in Fig. 2) and the trajectories which starting points lie on the horizontal axis in Fig. 2 at Y' and arbitrary z . We need to consider these two sets separately.

3.2 Solutions in Ω_1

In Ω_1 we need to use the initial condition $\phi(z = 0) = \phi_0$ to obtain the equation for $\mathcal{K}(\gamma_0)$.

$$\mathcal{K}(\gamma_0) = \frac{1}{\gamma_0} \left(-\mathcal{L}(\gamma_0) + \mathcal{F}(\gamma_0) e^{-\phi_0} + z_Y \right) \quad (3.8)$$

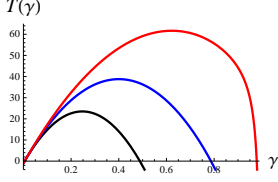


Fig. 4-a

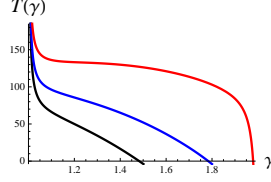


Fig. 4-b

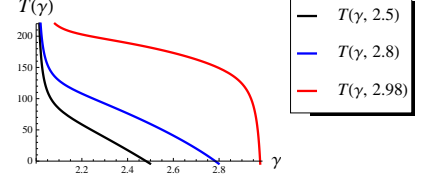


Fig. 4-c

Figure 4: $T(\gamma, \gamma_0)$ versus γ for $\gamma_0 = 0 \dots 1$ (Fig. 4-a), for $\gamma = 1 \dots 2$ (Fig. 4-b) and $\gamma = 2 \dots 3$ (Fig. 4-c) in the region Ω_1 . $N_0 = 0.1$ and $z_Y = 200$.

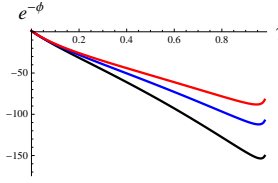


Fig. 5-a

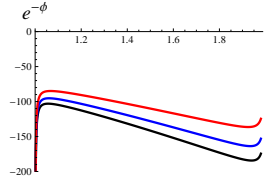


Fig. 5-b

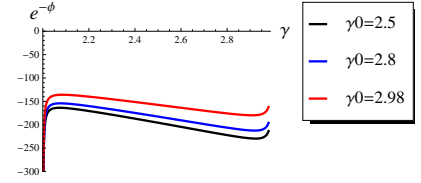


Fig. 5-c

Figure 5: $\exp(-\phi(\gamma, \gamma_0))$ versus γ for $\gamma_0 = 0 \dots 1$ (Fig. 5-a), for $\gamma = 1 \dots 2$ (Fig. 5-b) and $\gamma = 2 \dots 3$ (Fig. 5-c) in the region Ω_1 . $N_0 = 0.1$ and $z_Y = 200$.

Substituting Eq. (3.8) into Eq. (3.5)-Eq. (3.7) we have the final set of equations for the trajectories in the region Ω_1 .

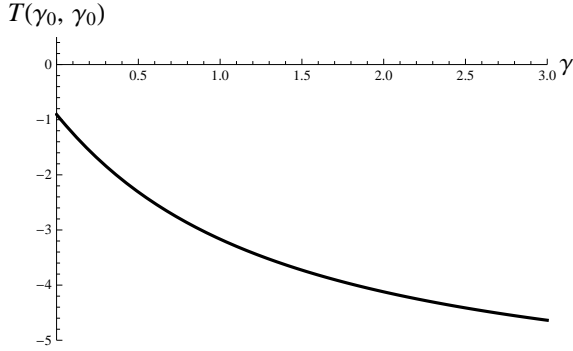


Figure 3: $T(\gamma_0, \gamma_0)$ versus γ_0 in the region Ω_1 . $N_0 = 0.1$ and $z_Y = 200$.

In Fig. 3 we see that function $\mathcal{T}(\gamma_0, \gamma_0)$ is negative for all values of γ_0 . It means that $\gamma(Y')$ falls down and becomes frozen at the value $\bar{\gamma}_0 = \gamma_{0,1}(\gamma_0)$ at which $T(\bar{\gamma}_0, \gamma_0) = 0$ (see Fig. 4). One can see that for $0 < \gamma < 1$ actually equation $T(\bar{\gamma}_0, \gamma_0) = 0$ has two solutions $\gamma_{0,1}$ and $\gamma_{0,2}$ but both are smaller than γ_0 . For $\gamma > 1$ we have the only one solution $\bar{\gamma}_0 < \gamma_0$. Actually, $\bar{\gamma}_0$ is very close to γ_0 . In other words, γ decreases very fast to $\bar{\gamma}_0$. At $\gamma = \bar{\gamma}_0$ $T(\gamma = \bar{\gamma}_0, \gamma_0) = 0$. Since the scattering amplitude N should be less than unity from the s -channel unitarity we expect that $\exp(-\phi(z, Y'))$ in entire kinematic

region should be positive and not equal to zero. Fig. 5 shows that we have a different behaviour of the solution for $\exp(-\phi(z(Y')))$ on the trajectories, which contradicts our expectation from the physics point of view.

Therefore, we can conclude that the semi-classical solution that satisfies the physical criterion, does

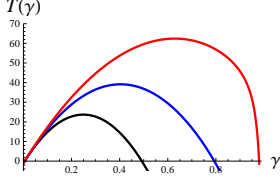


Fig. 7-a

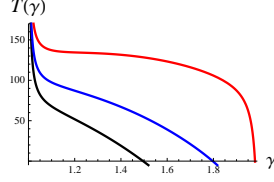


Fig. 7-b

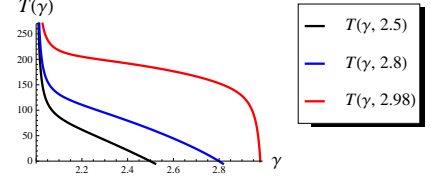


Fig. 4-c

Figure 7: $T(\gamma, \gamma_0)$ versus γ for $\gamma_0 = 0 \dots 1$ (Fig. 7-a), for $\gamma = 1 \dots 2$ (Fig. 7-b) and $\gamma = 2 \dots 3$ (Fig. 7-c) in the region Ω_2 . $N_0 = 0.1$ and $z_Y = 200$.

not exist at any γ_0 in the region Ω_1 when γ close to n with $n = 0, 1, 2, 3, \dots$

3.3 Solutions in Ω_2

In the region Ω_2 we have to repeat our analysis since the equation for $\mathcal{K}(\gamma_0)$ should be based on the initial condition: $\phi(z = z_0, Y' = 0) = \phi_0 \exp(z_0)$. Since $\gamma_0 = \phi(z = z_0, Y' = 0)$ for this initial condition Eq. (3.8) can be re-written in the form

$$\mathcal{K}(\gamma_0) = \frac{1}{\gamma_0} \left(-\mathcal{L}(\gamma_0) + \mathcal{F}(\gamma_0) e^{-\gamma_0} + z_Y \right) \quad (3.9)$$

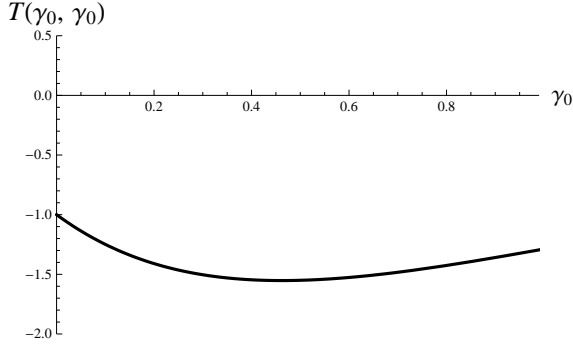


Figure 6: $T(\gamma_0, \gamma_0)$ versus γ_0 in the region Ω_2 . $N_0 = 0.1$ and $z_Y = 200$.

One can see in Fig. 6 that $T(\gamma_0, \gamma_0)$ in this region is negative. Therefore, in this region as in region Ω_1 $\gamma(z)$ falls down on the trajectory for all trajectories. It turns out that for each value of γ_0 function $T(\gamma, \gamma_0)$ vanishes at $\bar{\gamma}_0 = \gamma_{0,1}(\gamma_0)$ ($T(\bar{\gamma}_0, \gamma_0) = 0$) (see Fig. 7). Therefore, the solution in region Ω_2 has the same properties as the solution in region Ω_1 (see Fig. 7 and Fig. 8).

Thus we can repeat the same conclusions for the region Ω_2 as for Ω_1 : there is no solutions that satisfy the physical criteria.

4. Asymptotic solution with $\gamma \rightarrow z_Y / \left(\bar{\alpha}_S \frac{\chi(\gamma_{cr})}{1 - \gamma_{cr}} \right)$

Finally, the only solution which we need to consider is the solution with large $\gamma = d\phi(z, Y')/dz \rightarrow z_Y/C(\gamma_{cr}) \gg 1$. Eq. (2.23) reduces to the simple form

$$\frac{\partial \phi(z, Y')}{\partial \bar{\alpha}_S Y'} + C(\gamma_{cr}) \frac{\partial \phi(z, Y')}{\partial z} = z_Y \quad \text{where} \quad C(\gamma_{cr}) = \frac{\chi(\gamma_{cr})}{1 - \gamma_{cr}} \quad (4.1)$$

with the following initial conditions:

$$\phi(z = 0, Y') = \phi_0; \quad \phi(z, Y = 0') = \phi_0 e^z; \quad (4.2)$$

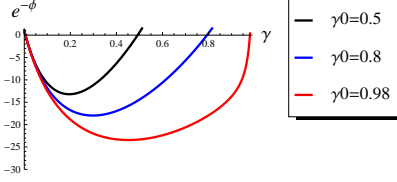


Fig. 8-a

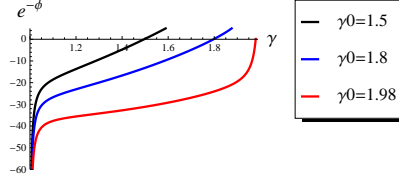


Fig. 8-b

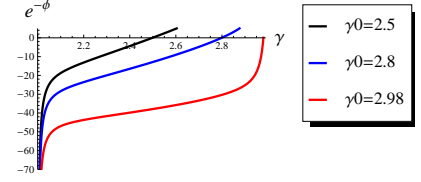


Fig. 8-c

Figure 8: $\exp(-\phi(\gamma, \gamma_0))$ versus γ for $\gamma_0 = 0 \dots 1$ (Fig. 8-a), for $\gamma = 1 \dots 2$ (Fig. 8-b) and $\gamma = 2 \dots 3$ (Fig. 8-c) in the region Ω_2 . $N_0 = 0.1$ and $z_Y = 200$.

We need to consider two separate kinematic regions Ω_1 and Ω_2 for searching the solutions for this equation (see Fig. 2): $Y' \geq z/C(\gamma_{cr})$ and $Y' \leq z/C(\gamma_{cr})$ [23]. In both regions the general solution to Eq. (4.1) takes the form

$$\phi(z, Y') = \frac{1}{2} z_Y (Y' + z/C(\gamma_{cr})) + G(Y' - z/C(\gamma_{cr})) \quad (4.3)$$

where G is the arbitrary function that has to be found from Eq. (4.2). In region Ω_2 one can see that

$$G_2 = \phi_0 \exp\left(-C(\gamma_{cr})(Y' - z/C(\gamma_{cr}))\right) \quad (4.4)$$

from the second of Eq. (4.2). However, in region Ω_1 we need to use the first of Eq. (4.2) and we obtain that

$$G_1 = -\frac{1}{2} z_Y (Y' - z/C(\gamma_{cr})) + \phi_0 \quad (4.5)$$

One can see that at $Y' = z/C(\gamma_{cr})$ two ϕ 's: $\phi_1(z) = z_Y z + \phi_0$ and $\phi_2(z, Y') = \frac{1}{2} z_Y (Y' + z/C(\gamma_{cr})) + \phi_0 \exp\left(-C(\gamma_{cr})(Y' - z/C(\gamma_{cr}))\right)$ are equal, providing the needed matching.

Therefore, the simplified Eq. (4.1) leads to the geometric scaling solution for $Y' \geq z/C(\gamma_{cr})$ while for $Y' \leq z/C(\gamma_{cr})$ we have a solution with explicit scaling violation.

Armed with the asymptotic solution given by Eq. (4.5) and Eq. (4.4) we study the numerical solution to Eq. (2.23) in region Ω_1 assuming the geometric scaling behaviour and considering the following iterative procedure. Plugging in Eq. (2.23) $\phi(z, Y') = \phi(z)$ and Eq. (2.31) we see that this equation takes the following form in this region

$$\frac{\chi(\gamma_{cr})}{1 - \gamma_{cr}} \frac{d\phi^{(i)}(z)}{dz} - 2 \left(\gamma_E + \ln \left(\frac{d\phi^{(i)}(z)}{dz} \right) \right) = z_Y - H(z) - H(z_Y - z) \quad \text{with} \quad H(z) = \int_0^z dz' e^{-\phi^{(i-1)}(z')} \quad (4.6)$$

where γ_E is the Euler constant ($\gamma_E = 0.5777216$) and where $\phi^{(i)}$ is the solution of the i -th iteration of the equation. Deriving Eq. (4.6) we used that $\tilde{\mathcal{L}} \xrightarrow{\gamma \gg 1} \gamma_E + \ln(\gamma)$.

We solve Eq. (4.6) using iteration procedure with

$$\phi^{(i=0)} = \left\{ (z_Y + 2(\gamma_E + \ln z_Y))(1 - \gamma_{cr})/\chi(\gamma_{cr}) \right\} z. \quad (4.7)$$

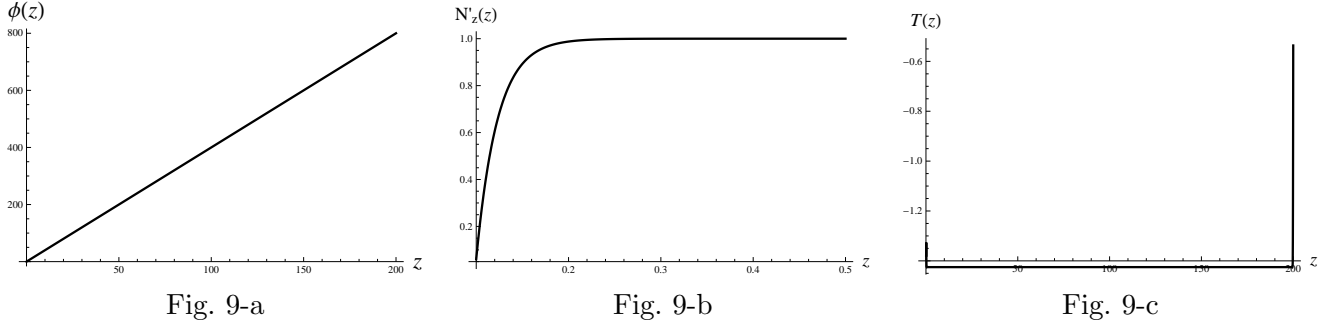


Figure 9: The third iteration of Eq. (4.6): solutions for functions $\phi(z)$ (Fig. 9-a) and the scattering amplitude $N'_z(z)$ (Fig. 9-b) versus z . In Fig. 9-c we plot function $T(z)$ (see Eq. (4.8)). In the figure the following parameters are taken: $N_0 = 0.1$ and $z_Y = 200$.

The result of the third iteration is shown in Fig. 9. One can see from Fig. 9-a that the solution is very close to $\phi^{(0)}$ given by Eq. (4.7). N'_z reaches the unitarity limit at small values of z ($z \leq 0.5$). In Fig. 9-c we plotted the difference between the l.h.s. and the r.h.s. of Eq. (2.23). This difference can be written in the form:

$$T^{(i)}(z) = \mathcal{L} \left(\phi_z^{(i)}(z) \right) - \mathcal{F} \left(\phi_z^{(i)}(z) \right) e^{-\phi^{(i)}(z)} - \tilde{N}^{(i)}(z) - \tilde{N}^{(i)}(z_Y - z) \quad (4.8)$$

where $e^{-\phi^{(i)}} = 1 - d\tilde{N}^{(i)}(z)/dz$ and $d\phi^{(i)}/dz = \frac{d^2 \tilde{N}^{(i)}(z)}{dz^2} / \left(1 - d\tilde{N}^{(i)}(z)/dz \right)$

$T^{(i)}(z)$ turns out to be small (less than 1) leading to the accuracy of the solution about 2%.

For the region Ω_2 (see Fig. 2) we solve a more general equation for $\phi(z, Y')$. In this case Eq. (4.6) takes the form

$$\frac{\partial \phi(z, Y')}{\partial \alpha_S Y'} + \frac{\chi(\gamma_{cr})}{1 - \gamma_{cr}} \frac{\partial \phi(z, Y')}{\partial z} - 2 \left(\gamma_E + \ln \left(\frac{d\phi(z, Y')}{dz} \right) \right) = z_Y + 4N_0 - H(z, Y') - H(z_Y - z, Y - Y') \quad (4.9)$$

where $H(z, Y') = \int_0^z dz' e^{-\phi(z', Y')}$. The initial conditions are given by Eq. (4.2).

The numerical solution is shown in Fig. 10. One can see that at large values of Y' solution approaches the geometric scaling solution of Eq. (4.6). We can use this physical solution, shown in Fig. 10 and Fig. 9, to study the N-N scattering in the next section.

5. Nucleus-nucleus scattering amplitude

We need to specify term S_E in Eq. (2.1) for calculating the scattering amplitude with a nucleus. This term determines the interaction of the BFKL Pomeron with the nucleons of the nucleus and it has been written in Ref. [1] in the following form

$$S_E = \int d^2b d^2k \left(\Phi(k, b, Y' = 0) \tau_{A_2}(k, b) + \Phi^\dagger(k, b, Y' = Y) \tau_{A_1}(k, b) \right) \quad (5.1)$$

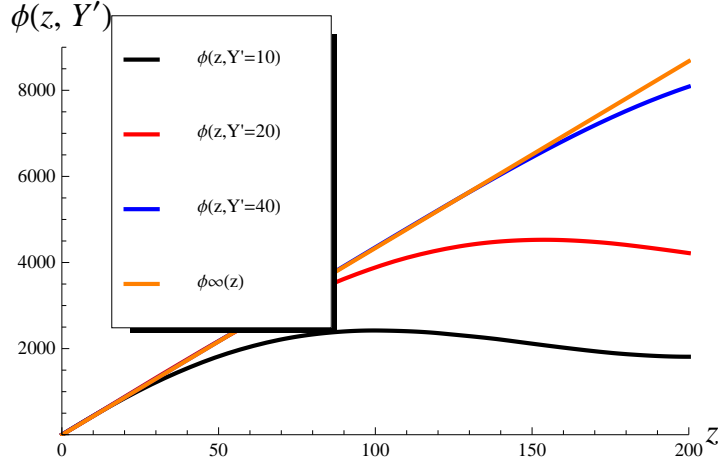


Figure 10: Function $\phi(z, Y')$ at different values of Y' as function of z . In the figure the following parameters are taken: $N_0 = 0.1$ and $z_Y = 200$

where

$$\tau_A(k, b) = S_A(b) \sigma(k) \quad \text{with} \quad S_A(b) = \int_{-\infty}^{+\infty} dz \rho(z, b) \quad \text{and} \quad \sigma(k) = \int n(k, b) d^2b \quad (5.2)$$

In Eq. (5.2) ρ is the density of the nucleons in the nucleus and $\sigma(k)$ is the cross section (imaginary part of the forward scattering amplitude) of the dipole with the nucleon at low energy while $n(k, b)$ is the dipole-nucleon scattering amplitude.

As we have eluded, in our treatment of nucleus-nucleus interaction we use the Glauber-type approach [26] integrating over all impact parameters of dipole-dipole and dipole-nucleon interaction since they are assumed to be much smaller than the impact parameters of nucleon-nucleon scattering (see for example Ref. [27] in which this approach is discussed in details). The latter is of the order of R_A , which is larger than the nucleon radius and the sizes of all interacting dipoles. As we have discussed, we assume that instead of the real nuclei we are dealing with the nuclei that consist of mesons made of heavy quark and antiquarks. For such mesons we can calculate $n(k)$ in the Born Approximation of perturbative QCD. In coordinate space $n(r) = (2\pi\alpha_S^2 C_F / N_c) r^2 \ln(R^2/r^2) \Theta(R - r)$ where R is the radius of the meson which is of the order of $1/(\alpha_S(M_Q) M_Q)$ where M_Q is the mass of heavy quark. In the momentum space we have the following $\tau_A(k, b)$

$$\tau_A(k, b) = S_A(b) \sigma(k) = S_A(b) \frac{\alpha_S^2 C_F}{\pi N_c} \frac{1}{k^2 + \alpha_S^2 M_Q^2} \quad (5.3)$$

τ determine the initial conditions for the amplitude $N(k, b, Y')$ and $N^\dagger(k, b, Y')$, namely

$$N(k, b, Y' = 0) = \tau_{A_1}(b, k); \quad N^\dagger(k, b, Y' = Y) = \tau_{A_2}(b, k); \quad (5.4)$$

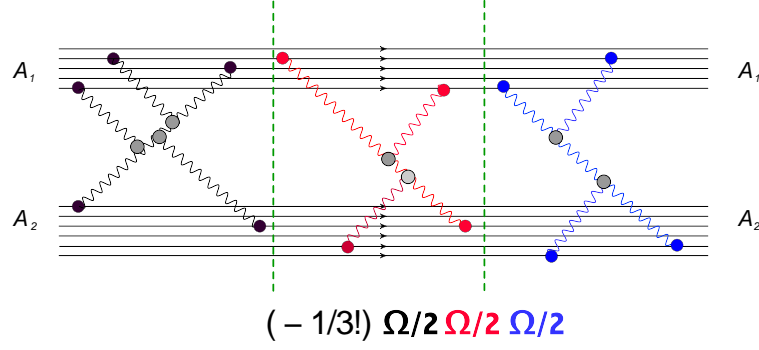


Figure 11: The example of two nuclei reducible diagram in the scattering amplitude for nucleus-nucleus interaction.

For simplicity, we consider the cylindric nuclei for which the b dependence is given by $\Theta(R_A - b)$. In this model

$$S_A(b) = 2\rho_0 R_A \Theta(R_A - b) \quad (5.5)$$

In this simple model the entire b dependence of $N(k, b, Y')$ and $N^\dagger(k, b, Y')$ turns out to be the same as in initial condition leading to

$$\begin{aligned} N(k, b, Y') &= S_A(b) \sigma(k, Y') = S_A(b) \frac{1}{k_0^2} \mathcal{N}(k, Y') \\ N^\dagger(k, b, Y') &= S_A(b) \sigma^\dagger(k, Y') = S_A(b) \frac{1}{k_0^2} \mathcal{N}^\dagger(k, Y') \end{aligned} \quad (5.6)$$

where k_0 is the typical transverse momentum in the proton ($k_0 \propto \alpha_S M_Q$). Functions \mathcal{N} and \mathcal{N}^\dagger are dimensionless and for them we have the geometric scaling behaviour inside the saturation region [20] and in the vicinity of the saturation outside of the saturation region [19].

Using $\rho(z=0, b=0) = \rho_0 = 0.171/fm^3$ and $R_A = 1.2 A^{1/3} fm$ we can estimate the value of τ at $k=0$ for the gold: $\tau = 8\rho_0 R_A/(9\pi M_Q^2) = 0.32(1/fm^2)/M_Q^2$. One can see that $N_0 = 0.1$ which we used for the numerical solution can be reached even at $k=0$ if $M_Q \approx 0.36 GeV$.

Calculating the scattering amplitude, we need first to sum all two nuclei reducible diagrams (see Fig. 11 for example). In such diagrams we can single out one or more states with two nuclei in the s -channel (see, for example, two such states in Fig. 11).

This sum can be written as follows

$$ImA(b, Y) = \left(1 - e^{-\frac{1}{2}\Omega(b, Y)}\right) \quad (5.7)$$

The notation : Ω in Eq. (5.7), is introduced to be opacity for the nucleus-nucleus scattering in the Glauber-Gribov approach [26].

Using Eq. (5.1) one can see that the equation for the opacity Ω has the following form (see Fig. 12)

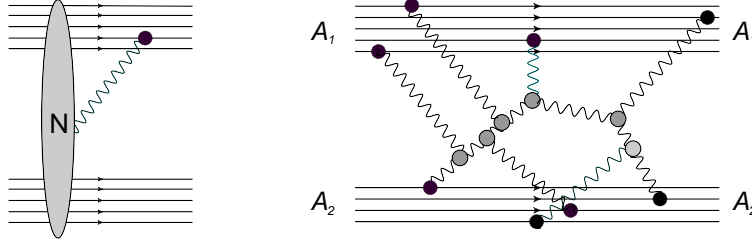


Figure 12: The equation for opacity Ω .

$$\Omega(b, Y) = \int d^2b' d^2k \tau_{A_1}(\vec{b} - \vec{b}', k) N(b', k, Y' = Y) = \int d^2b' d^2k N^\dagger(\vec{b} - \vec{b}', k, Y' = 0) \tau_{A_2}(b', k) \quad (5.8)$$

Plugging in Eq. (5.6) we can rewrite Eq. (5.8) in the form

$$\Omega(b, Y) = T_{AA}(b) \int d^2k \sigma(\vec{b} - \vec{b}', k) \sigma(k, Y' = Y) = T_{AA}(b) \frac{1}{k_0^2} \int d^2k \sigma(\vec{b} - \vec{b}', k) \mathcal{N}(k, Y' = Y) \quad (5.9)$$

where

$$\begin{aligned} T_{AA}(b) &= (2\rho_0 R_A)^2 \int d^2b' \Theta(b' - R_A) \Theta(|\vec{b} - \vec{b}'| - R_A) \\ &= (2\rho_0 R_A)^2 R_A^2 \left(2 \arccos\left(\frac{b}{2R_A}\right) - \frac{b}{2R_A} \sqrt{1 - \frac{b^2}{4R_A^2}} \right) \end{aligned} \quad (5.10)$$

As we have discussed the solution for $\mathcal{N}(z)$ at $z \leq z_{min}$ and $\mathcal{N}^\dagger(Z_Y - z)$ for $z_Y - z \leq z_{min}$ are the solution to the linear BFKL equation which can be written in the following form

$$\begin{aligned} 0 \leq z \leq z_{min} \quad N(k, Y) &= \frac{1}{k_0^2} \mathcal{N}(z) = \int d^2k' \sigma(k') \sigma_{BFKL}(k/k', Y' = Y) \\ &= \frac{\alpha_S^2 C_F}{\pi N_c} \frac{1}{k_0^2} \int \frac{dk'^2}{k'^2 + \alpha_S^2 M_Q^2} \mathcal{N}_{BFKL}(k/k', Y' = Y) \end{aligned} \quad (5.11)$$

$$\begin{aligned} 0 \leq z_Y - z \leq z_{min} \quad N^\dagger(k, Y) &= \frac{1}{k_0^2} \mathcal{N}^\dagger(z) = \int d^2k' \sigma(k') \sigma_{BFKL}^\dagger(k/k', Y' = Y) \\ &= \frac{\alpha_S^2 C_F}{\pi N_c} \frac{1}{k_0^2} \int \frac{dk'^2}{k'^2 + \alpha_S^2 M_Q^2} \mathcal{N}_{BFKL}^\dagger(k/k', Y' = Y) \end{aligned} \quad (5.12)$$

In the vicinity of the saturation scale \mathcal{N}_{BFKL} and $\mathcal{N}_{BFKL}^\dagger$ in Eq. (5.11) and Eq. (5.12) can be written in the simple form [20]:

$$\mathcal{N}_{BFKL}(k/k', Y' = Y) = N_0 e^{(1-\gamma_{cr})z'} \quad \text{and} \quad \mathcal{N}_{BFKL}^\dagger(k/k', Y' = Y) = N_0 e^{(1-\gamma_{cr})(z_Y - z')} \quad (5.13)$$

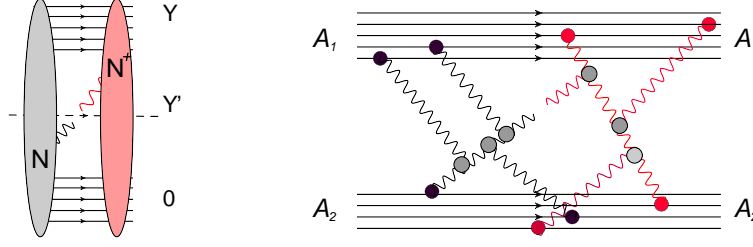


Figure 13: Graphic form of Eq. (5.16). Solid black lines denote the Pomerons and their interactions that contribute to N , while the same contributions for N^\dagger are shown in red.

where

$$z' = \bar{\alpha}_S \frac{\chi(\gamma_{cr})}{1 - \gamma_{cr}} Y - \ln(k^2/k'^2) \quad (5.14)$$

Taking the integration over k' in Eq. (5.11) and Eq. (5.12) we obtain:

$$\begin{aligned} 0 \leq z \leq z_{min} \quad \mathcal{N}(z) &= \frac{\alpha_S^2 C_F}{\pi N_c} \frac{N_0}{1 - \gamma_{cr}} \exp\left((1 - \gamma_{cr})z\right) \\ 0 \leq z_Y - z \leq z_{min} \quad \mathcal{N}^\dagger(z) &= \frac{\alpha_S^2 C_F}{\pi N_c} \frac{N_0}{1 - \gamma_{cr}} \exp\left((1 - \gamma_{cr})(z_Y - z)\right) \end{aligned} \quad (5.15)$$

It should be noticed that in the above equations l is defined as $l = \ln(k^2/(\alpha_S M_Q)^2)$ (see Eq. (2.18) and Eq. (2.11)) with $k_0^2 = (\alpha_S M_Q)^2$.

Having these equation in mind we use a generalization of Eq. (5.9)

$$\Omega(b; Y) = T_{AA}(b) \int dl \mathcal{N}^\dagger(Y - Y'; L - l) \mathcal{N}(Y'; l) \quad (5.16)$$

Eq. (5.16) has been proposed and discussed in Ref. [17] and for the nucleus-nucleus scattering it is illustrated by Fig. 13. From this figure one can see that arbitrary BFKL Pomeron diagram for the case of nucleus-nucleus scattering can be written as the product of $N^\dagger N$. The extra Pomeron contribution that could connect two sets of diagrams for N^\dagger and N (shown in black for N and in red for N^\dagger in Fig. 13) leads to a small corrections (see Ref. [4] for details). Y' is the arbitrary rapidity which is chosen from the condition $z = z_{min}$.

Using Eq. (4.4) for $\mathcal{N}^\dagger(Y - Y'; L - l)$ we can reduce Eq. (5.16) to the form

$$\Omega(b, z_Y) = T_{AA}(b) \frac{\alpha_S^2 C_F}{\pi N_c (\alpha_S M_Q)^2} \frac{N_0}{1 - \gamma_{cr}} \int_{z_Y + z_{min}} dz e^{(1 - \gamma_{cr})(z_Y - z)} \mathcal{N}(z) \quad (5.17)$$

This equation stems from the geometric scaling behaviour of the solution to the equations for N and N^\dagger .

In the kinematic region $z \leq 2z_{min}$ both \mathcal{N} and \mathcal{N}^\dagger in Eq. (5.16) are the solution of the BFKL equation and Ω in this region can be written as follows using Eq. (2.12):

$$z_Y \leq 2 z_{min} : \quad \Omega(b, z_Y) = \frac{T_{AA}(b)}{(\alpha_S M_Q)^2} \left(\frac{\alpha_S^2 C_F}{\pi N_c} \right)^2 \frac{N_0^2}{(1 - \gamma_{cr})^2} \exp((1 - \gamma_{cr}) z_Y) \quad (5.18)$$

For large $z > 2 z_{min}$ $N(z)$ is given by solution of Eq. (4.6). For estimates we can use for $N(z)$ in this region the solution in the form

$$\mathcal{N}_{z > z_{min}}(z) = \int_{z_{min}}^z dz' \left(1 - e^{-\phi^{(i=0)}(z')} \right) + \mathcal{N}(z_{min}) \quad (5.19)$$

where $\phi^{(i=0)}$ is given by Eq. (4.7). The expression for Ω reads as follows

$$\begin{aligned} z_Y \geq 2 z_{min} : \quad \Omega(b, z_Y) = & \frac{T_{AA}}{(\alpha_S M_Q)^2} \left(\frac{\alpha_S^2 C_F}{\pi N_c} \right)^2 \frac{N_0}{1 - \gamma_{cr}} \left\{ \int_{z_{min}}^{z_Y - z_{min}} dz \int_{z_{min}}^z dz' \left(1 - e^{-\phi^{(i=0)}(z')} \right) \right. \\ & \left. + \frac{N_0}{(1 - \gamma_{cr})} \exp\left(2(1 - \gamma_{cr}) z_{min} \right) \right\} \end{aligned} \quad (5.20)$$

The result of our estimates using Eq. (5.18) - Eq. (5.20) is plotted in Fig. 14. One can see that starting with small values of $z_Y \geq 8$ the amplitude at $b = 0$ is close to the unitarity bound (see red line in Fig. 11). For comparison we plot in Fig. 14 also the amplitude which corresponds to the exchange by one BFKL Pomeron in nucleon-nucleon scattering:

$$A_P(AA; z_Y, b) = i \left(1 - \exp \left(-\frac{1}{2} \Omega_P(z_Y, b) \right) \right) \quad (5.21)$$

with $\Omega_P(z_Y, b)$ given by Eq. (5.11) at any value of z_Y .

The main conclusions that we can make from Fig. 14 is the fact that the exact solution for nucleus-nucleus scattering shows the same corrections as Glauber-Gribov formula. This happens because at $z_Y = 2z_{min}$ the amplitude turns out to be very close to the unitarity bound. However, it should be stress that actually the exact solution leads to slower approaching to the unitarity bound since it turns out (see Fig. 15) that $\Omega(z_Y, b)$ of Eq. (5.17) is much smaller than $\Omega_P(z_Y, b)$ of Eq. (5.18) that corresponds to the exchange of one BFKL Pomeron at the entire kinematic region.

6. Conclusions

The main result of this paper is the solution in the form of Eq. (2.21) for amplitude $N(Y, Y', l) = N(z, Y')$ with $\phi(z, Y')$ given by Eq. (4.3) and Eq. (4.6) and with the initial function $\phi^{(0)}(z, Y')$ determined by Eq. (4.2). We obtained this solution in two steps. First, we assume that Eq. (2.14) ($N(l, b; Y; Y_0) = N^\dagger(b; L - l, Y - Y_0)$) which is correct for the linear equation, is valid for the solution of the non-linear one. This conjecture allows us to reduce the system of two equations to one functional differential equation. Second, we solve this equation. The semi-classical approach was used to select out the infinite number of parasite solutions and the final solution was found analytically at large values of Y' as well as numerically in the entire region of Y' .

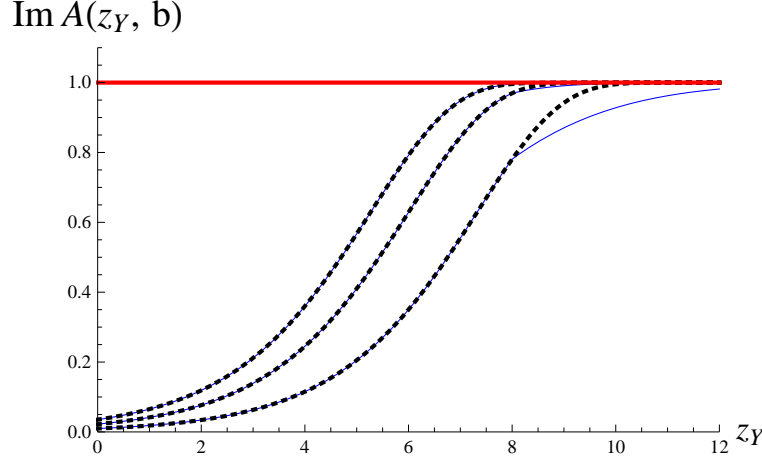


Figure 14: The scattering amplitude for gold-gold interaction versus $z \equiv z_Y$ at different values of b : the solid black line is the result of this paper (see Eq. (5.20)), the red dotted curve describes the Glauber-Gribov formula for one BFKL Pomeron exchange (see Eq. (5.21)); and the red line shows the unitarity bound. The curves correspond $b = 0, 5 \text{ fm}$ and 10 fm going from left to right,

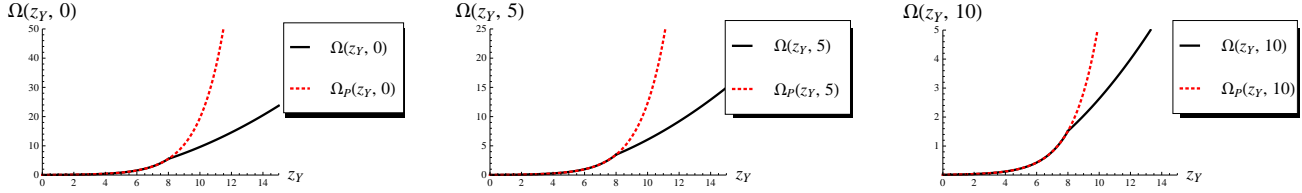


Figure 15: The opacity $\Omega(z_Y, b)$ of Eq. (5.20) and $\Omega_P(z_Y)$ of Eq. (5.11) for gold-gold interaction at different b versus $z \equiv z_Y$: black line is the result of this paper (see Eq. (5.18)), the red dotted curve describes the contribution to Ω from exchange of one BFKL Pomeron. The values of b are given in *fermi*.

The solution, that has been found, looks as being different from the numerical solutions found in Refs. [2,3], but it shares with them several common features. In particular, this solution exists only and $z \leq z_{min} \approx 4$. In our solution the amplitude $N^\dagger(Y, Y', l) = N(z_Y - z)$. We have no proof that this solution is unique but we believe that the physics problem has the only one solution.

Using this solution we found the nucleus-nucleus scattering amplitude as a function of energy for ‘theoretical’ nuclei. This ‘theoretical’ nucleus consists of the dipoles that are made of heavy quarks and antiquarks. We can use the perturbative QCD treating this nucleus. In reconstruction of the scattering amplitude we use Eq. (5.16) (see Fig. 12) which is the form of t -channel unitarity constraints and follows from Eq. (5.1) for S_E term in the action of Eq. (2.1).

We showed that for $z_Y \leq 2z_{min}$ the exact calculation give the same result as the Glauber-Gribov formula which is widely used for nucleus-nucleus scattering. It turns out that $z_{min} \approx 4$ is so large that our estimates lead to the result close to the Glauber-Gribov formula in the entire kinematic region of energies. Only at large impact parameters the exact formula for nucleus-nucleus scattering gives visible deviations

from the estimates based on Glauber-Gribov approach. We believe that this observation is important for all practical estimates based on Glauber-Gribov approach.

In spite of the fact that the solved problem is still far away from the real physics environment we hope that our solution gives a reasonable first approximation to approach the nucleus-nucleus scattering for the nuclei that exist in reality.

7. Acknowledgements

We thank all participants of the HEP seminar at UTFSM for useful discussions. This research was supported by the Fondecyt (Chile) grants 1100648, 1095196 and DGIP 11.11.05.

References

- [1] M. A. Braun, Phys.Lett. B 483 (2000) 115, [arXiv:hep-ph/0003004]; Eur.Phys.J C **33** (2004) 113 [arXiv:hep-ph/0309293]; Phys. Lett. B **632** (2006) 297, [Eur. Phys. J. C **48** (2006) 511], [arXiv:hep-ph/0512057].
- [2] S. Bondarenko and L. Motyka, Phys. Rev. D **75** (2007) 114015 [arXiv:hep-ph/0605185].
- [3] S. Bondarenko and M. A. Braun, Nucl. Phys. A **799** (2008) 151 [arXiv:0708.3629 [hep-ph]].
- [4] A. Kormilitzin, E. Levin, J. S. Miller, Nucl. Phys. **A859** (2011) 87-113. [arXiv:1009.1329 [hep-ph]].
- [5] C. Contreras, E. Levin and J. S. Miller, Nucl. Phys. A **880** (2012) 29 [arXiv:1112.4531 [hep-ph]].
- [6] S. Bondarenko, M. Kozlov, E. Levin, Nucl. Phys. **A727** (2003) 139-178, [hep-ph/0305150] and references therein.
- [7] L. V. Gribov, E. M. Levin and M. G. Ryskin, Phys. Rep. **100** (1983) 1.
- [8] A. H. Mueller and J. Qiu, Nucl. Phys. **B268** (1986) 427.
- [9] L. McLerran and R. Venugopalan, Phys. Rev. **D49** (1994) 2233, 3352; **D50** (1994) 2225; **D53** (1996) 458; **D59** (1999) 09400.
- [10] A. H. Mueller, Nucl. Phys. B **415**, 373 (1994); Nucl. Phys. B **437** (1995) 107 [arXiv:hep-ph/9408245].
- [11] I. Balitsky, [arXiv:hep-ph/9509348]; *Phys. Rev.* **D60**, 014020 (1999) [arXiv:hep-ph/9812311]; Y. V. Kovchegov, *Phys. Rev.* **D60**, 034008 (1999), [arXiv:hep-ph/9901281].
- [12] J. Jalilian-Marian, A. Kovner, A. Leonidov and H. Weigert, *Phys. Rev.* **D59**, 014014 (1999), [arXiv:hep-ph/9706377]; *Nucl. Phys.* **B504**, 415 (1997), [arXiv:hep-ph/9701284]; J. Jalilian-Marian, A. Kovner and H. Weigert, *Phys. Rev.* **D59**, 014015 (1999), [arXiv:hep-ph/9709432]; A. Kovner, J. G. Milhano and H. Weigert, *Phys. Rev.* **D62**, 114005 (2000), [arXiv:hep-ph/0004014]; E. Iancu, A. Leonidov and L. D. McLerran, *Phys. Lett.* **B510**, 133 (2001); [arXiv:hep-ph/0102009]; *Nucl. Phys.* **A692**, 583 (2001), [arXiv:hep-ph/0011241]; E. Ferreira, E. Iancu, A. Leonidov and L. McLerran, *Nucl. Phys.* **A703**, 489 (2002), [arXiv:hep-ph/0109115]; H. Weigert, *Nucl. Phys.* **A703**, 823 (2002), [arXiv:hep-ph/0004044].

- [13] L. McLerran, Nucl. Phys. A **862-863**, 251 (2011) [arXiv:1105.4097 [hep-ph]]; Prog. Theor. Phys. Suppl. **187** (2011) 17 [arXiv:1011.3204 [hep-ph]]; Int. J. Mod. Phys. A **25** (2010) 5847 [arXiv:0812.1518 [hep-ph]]; F. Gelis, E. Iancu, J. Jalilian-Marian and R. Venugopalan, Ann. Rev. Nucl. Part. Sci. **60** (2010) 463 [arXiv:1002.0333 [hep-ph]]; F. Gelis, T. Lappi and R. Venugopalan, Int. J. Mod. Phys. E **16** (2007) 2595 [arXiv:0708.0047 [hep-ph]].
- [14] E. A. Kuraev, L. N. Lipatov, and F. S. Fadin, *Sov. Phys. JETP* **45**, 199 (1977); Ya. Ya. Balitsky and L. N. Lipatov, *Sov. J. Nucl. Phys.* **28**, 22 (1978).
- [15] L. N. Lipatov, Phys. Rep. **286** (1997) 131; Sov. Phys. JETP **63** (1986) 904 and references therein. ep-ph]].
- [16] J. Bartels and K. Kutak, Eur. Phys. J. C **53**, 533 (2008). [arXiv:0710.3060 [hep-ph]] and references therein.
- [17] A. H. Mueller and A. I. Shoshi, Nucl. Phys. B **692** (2004) 175 [arXiv:hep-ph/0402193].
- [18] A. H. Mueller and D. N. Triantafyllopoulos, *Nucl. Phys.* **B640** (2002) 331 [arXiv:hep-ph/0205167]; D. N. Triantafyllopoulos, *Nucl. Phys.* **B648** (2003) 293 [arXiv:hep-ph/0209121].
- [19] E. Iancu, K. Itakura, L. McLerran, Nucl. Phys. **A708** (2002) 327-352. [hep-ph/0203137]
- [20] J. Bartels, E. Levin, Nucl. Phys. **B387** (1992) 617-637; A. M. Stasto, K. J. Golec-Biernat, J. Kwiecinski, Phys. Rev. Lett. **86** (2001) 596-599, [hep-ph/0007192]; L. McLerran, M. Praszalowicz, Acta Phys. Polon. **B42** (2011) 99, [arXiv:1011.3403 [hep-ph]] **B41** (2010) 1917-1926, [arXiv:1006.4293 [hep-ph]]. M. Praszalowicz, [arXiv:1104.1777 [hep-ph]], [arXiv:1101.0585 [hep-ph]].
- [21] E. Levin and K. Tuchin, Nucl. Phys. B **573** (2000) 833 [arXiv:hep-ph/9908317].
- [22] P.Hartman, “ Ordinary differential equations”, second ed., Birkhäuser, Boston-Basel-Stuttgart, 1982.
- [23] A. Kormilitzin, E. Levin and S. Tapia Nucl. Phys. A **872** (2011) 245 [arXiv:1106.3268 [hep-ph]].
- [24] E. M. Levin and M. G. Ryskin, Yad. Fiz. **45** (1987) 234 [Sov. J. Nucl. Phys. **45** (1987) 150].
- [25] Y. V. Kovchegov and H. Weigert, Nucl. Phys. A **789** (2007) 260 [hep-ph/0612071].
- [26] R.J. Glauber, In: Lectures in Theor. Phys., v. 1, ed. W.E. Brittin and L.G. Duham. NY: Intersciences, 1959; V. N. Gribov, Sov. Phys. JETP **29** (1969) 483 [Zh. Eksp. Teor. Fiz. **56** (1969) 892].
- [27] E. Levin, J. Miller, B. Z. Kopeliovich and I. Schmidt, JHEP **0902** (2009) 048 [arXiv:0811.3586 [hep-ph]].